Supplementary material

1. Sampling protocol

In each site, three points located approximately 200 meters apart were sampled (Figure 1a and 1b of the article). In the intertidal, each point was sampled using three sets of three sediment cores totalling 0.03 m^2 while in the subtidal, macrofauna was collected at each of the three points using three Smith-McIntyre grabs of 0.1 m^2. These nine cores or grabs were then pooled to estimate abundances at the site level. Accordingly, macrofaunal densities were estimated based on 0.27 m^2 and 0.9 m^2 surfaces sampled per site for the intertidal and subtidal sites respectively. The exact number of sediment cores or grabs used for each sampling occasion is summarized in Figure S1. Each core and grab sample was sieved over 1 mm mesh and fixed in 4% formalin solution until sorting and morphological identification to the lowest possible taxonomic levels in the laboratory. Homogenization of the taxonomy was performed as described in Boyé et al. (2017) to ensure a consistent taxonomic resolution across sites and years.

2. Biological and ecological processes associated to each trait

Table S1 List of traits and associated biological and ecological processes.

Trait	Biological and ecological processes associated
Maximum size (mm)	Resource acquisition, habitat use, species interaction (competition, predation), nutrient cycling, secondary production (Degen et al., 2018; Törnroos & Bonsdorff, 2012)
Feeding method	Resource utilisation, energy transfer, nutrient cycling (Törnroos & Bonsdorff, 2012)
Food size	Resource utilisation, energy transfer, nutrient cycling (Törnroos & Bonsdorff, 2012)
Adult preferred substrate position	Resource acquisition, habitat use, species interaction, nutrient cycling (Norling et al., 2007; Törnroos & Bonsdorff, 2012)
Living habit	Colonisation, recovery dynamics, dispersal, nutrient cycling (Norling et al., 2007; Queirós et al., 2013)
Daily adult movement capacity	Colonisation, recovery dynamics, dispersal (Törnroos & Bonsdorff, 2012)
Bioturbation	Nutrient cycling, sediment oxic-anoxic boundaries and chemical properties (Norling et al., 2007; Queirós et al., 2013) ; species interaction (Bouma et al., 2009)
Sexual differentiation	Recovery dynamics, dispersal, secondary production (Törnroos & Bonsdorff, 2012)
Development mode	Recovery dynamics, dispersal, secondary production (Törnroos & Bonsdorff, 2012)
Reproduction frequency	Recovery dynamics, dispersal, secondary production (Törnroos & Bonsdorff, 2012)
Life span	Secondary production, recovery dynamics, dispersal (Degen et al., 2018)

3. Imputation of missing trait data

Overall, data on maximum life span were missing for half of the species so that it was removed from analyses. For the reproduction frequency, development mode, and sexual differentiation, data were missing for 9% (21 species), 7% (17), and 1% (3) of the species respectively. For these traits, we imputed missing values using nearest neighbour imputation relying on Gower dissimilarity that accommodates missing data. Missing traits were imputed based on the median value of the functionally closest species for which the trait was known as well as those falling within a threshold dissimilarity of 0.01 times the dissimilarity between this closest species and the species to be inferred. This procedure gave similar results to imputation based on the 5 nearest neighbours using the *kNN* function of the *VIM* package in R (Kowarik & Templ, 2016). The species used to infer each missing data were then verified by experts of benthic taxonomy to ensure the ecological soundness of this imputation procedure.

4. Description of the coding scheme with examples

In our coding procedure, a species expresses each modality of a given trait on a scale from 0 to 4, with 4 being an exclusive affinity for a modality (all other modalities of the trait being 0 for that species), 3 a strong affinity for a modality, 2 a mean or uncertain affinity for a modality, 1 an occasional behaviour or observed value for the species, and 0 for the absence of the modality. When the species expressed several modalities of a trait without marked preferences, or with unknown preferences, it

was coded 2 for all modalities expressed and 0 for those not expressed. On the other hand, when species expressed marked preferences for some modalities of a trait while expressing others occasionally, the preferred modalities were coded 3, the occasional modalities were coded 1 and those not expressed were coded 0. This coding procedure accounts to some extent for the plasticity of species and allows a rough incorporation of within-species variability in the functional analysis, which is known to have an important role in benthic ecosystem functioning (Wohlgemuth et al., 2017).

Table S2 Practical examples of the fuzzy coding procedure used in this study.

Known affinity of the species	Modality A	Modality B	Modality C	Modality D
Only modality A expressed	4	0	0	0
Affinity shared between modality A and B without marked or known preferences	2	2	0	0
Mainly expresses modality A (strong affinity), and occasionally expresses modality B	3	1	0	0
Mainly expresses modality A but also modality B, with a preference less marked that in the case above	3	2	0	0
Mainly expresses modality A, but occasionally expresses modality B and C	3	1	1	0
Mainly expresses modality A, but also modality B, and occasionally modality C	3	2	1	0

5. Functional α diversity indices

5.1. Description of the functional indices and their complementarity

The *FRic* corresponds to the convex hull volume occupied by the species of an assemblage in the multidimensional trait space, which is used as a measure of the size of the niche space occupied by an assemblage (Blonder, 2017; Cornwell et al., 2006). It is the multidimensional equivalent of the trait range, and is unaffected by species abundances (Schleuter et al., 2010; Villéger et al., 2008). The three other indices on the other hand, inform on abundances distribution in the trait space. *FEve* measures the regularity of species abundances within the convex hull volume, accounting for both the evenness of abundance distribution among species and for the regularity of the functional distances among species (Villéger et al., 2008). *FDiv* is the abundance-weighted deviations of species to the species' mean distance to the centre of gravity of the convex hull (Schleuter et al., 2010). It describes whether high abundances are distributed in the centre or in the external part of the trait space occupied by the assemblage, or in other words, whether the most abundant species have the most extreme traits or have on the contrary average characteristics. Two important properties of this index are that species abundances are not involved in the calculation of the coordinates of the centre of gravity of the convex hull and that the size of the functional space does not influence its value (Villéger et al., 2008). In contrast, *FDis* accounts for the size of the functional space occupied by the assemblages and species abundances are involved in all steps of the calculation as it is defined as the abundance-weighted mean distance of species to their abundance-

weighted centroid (Laliberté & Legendre, 2010). Therefore, these four indices are rather independent from each other and provide insights into different aspects of the functional structure of the assemblages (Laliberté & Legendre, 2010; Mouchet et al., 2010).

5.2. Method used for their calculation

$FRic$, $FEve$, and $FDiv$ were computed on a subset of Principal Coordinates Analysis (PCoA) axes following Villéger et al. (2008) and Laliberté & Legendre (2010). Euclidean distance was computed on the standardised species-by-trait matrix and PCoA was performed after removing assemblages with less than 5 species, in order to keep 5 PCoA axes for the calculation of the indices. This allowed the calculation of the $FEve$ (at least three species are needed, Villéger et al., 2008) and resulted in a reduced-space that represented 66% of the original variance (quality of the representation measured with R^2-like ratio as described in Legendre & Legendre, 2012, p. 505–506). This reduction of dimensionality to 5 axes is often done to ease the calculation of convex hull volumes and has been suggested to be sufficient to characterise most ecological systems (Blonder, 2017).

6. Figures

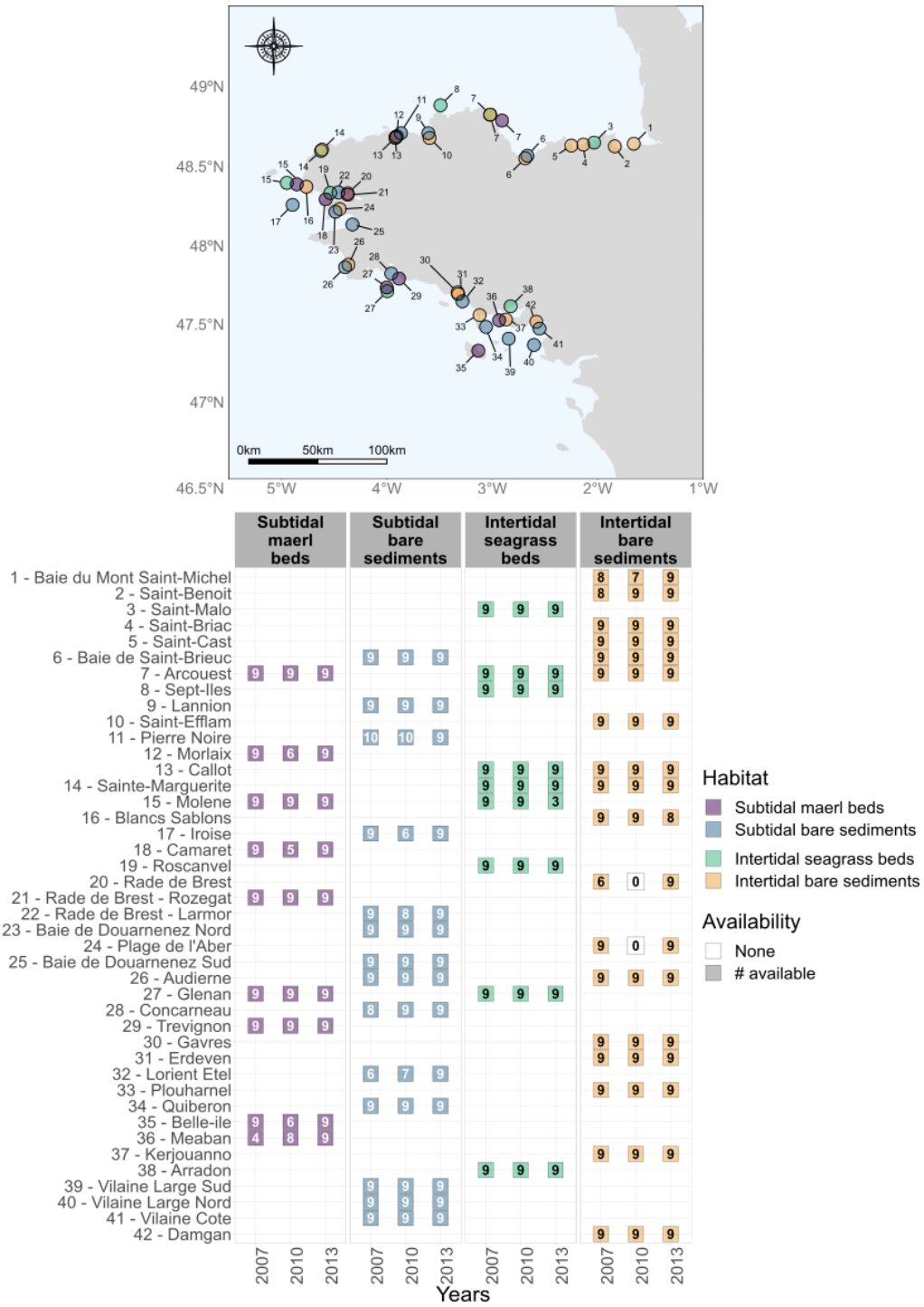

Figure S1 Number of grab or core samples available for the different sites for the three years of the study. Only one site of bare subtidal sediments (11-Pierre Noire) did not follow the same protocol than other locations with the sampling of ten grabs located in a single point instead of nine grabs in three separated points

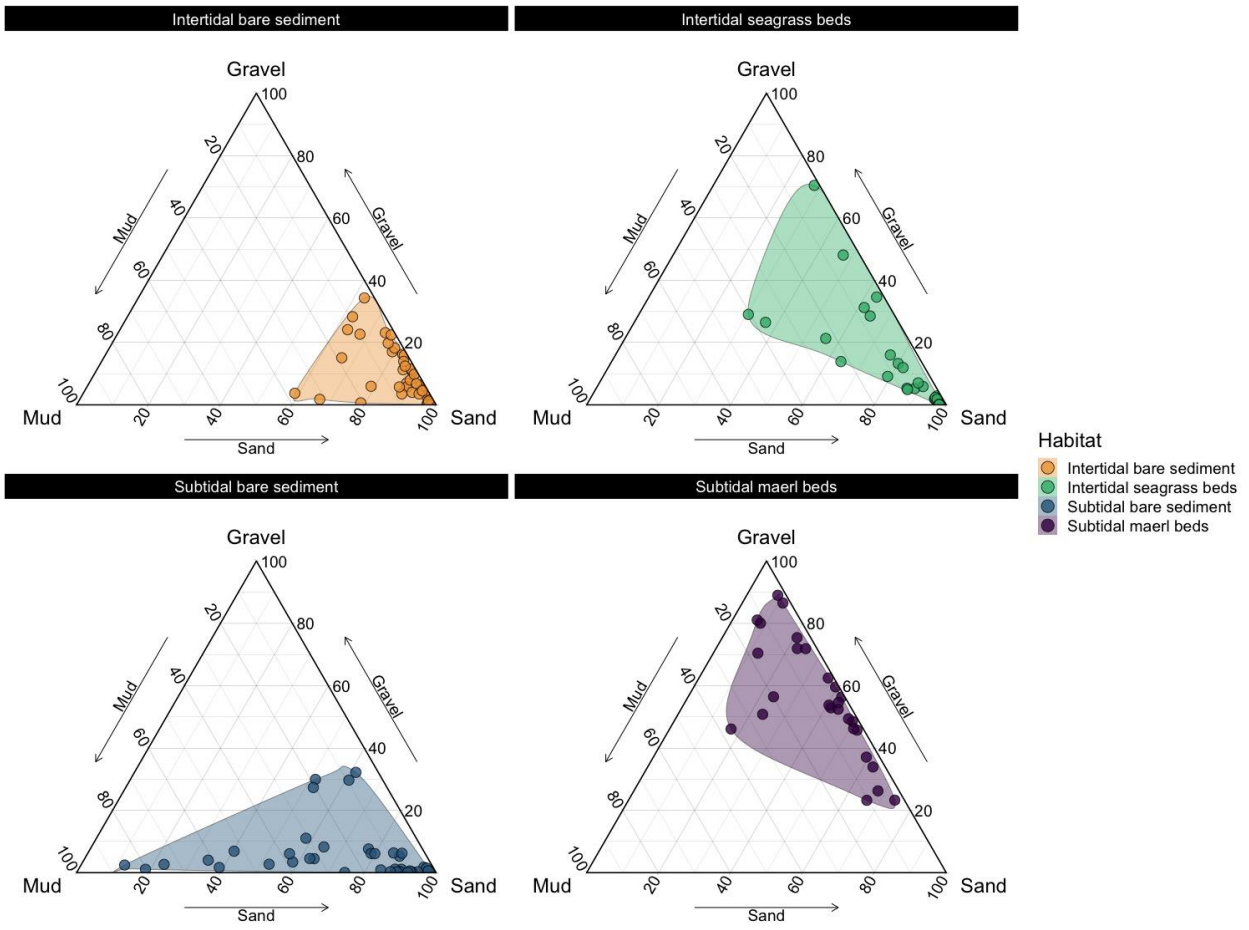

Figure S2 Variability of the granulometry of the sediment across locations and habitats. The grain size distribution of the sediment was grouped into three fractions: gravels (> 2 mm), sand (63 µm to 2 mm) and mud (< 63 µm). Each point represents the granulometry of a given site for a given year with colours corresponding to the habitat

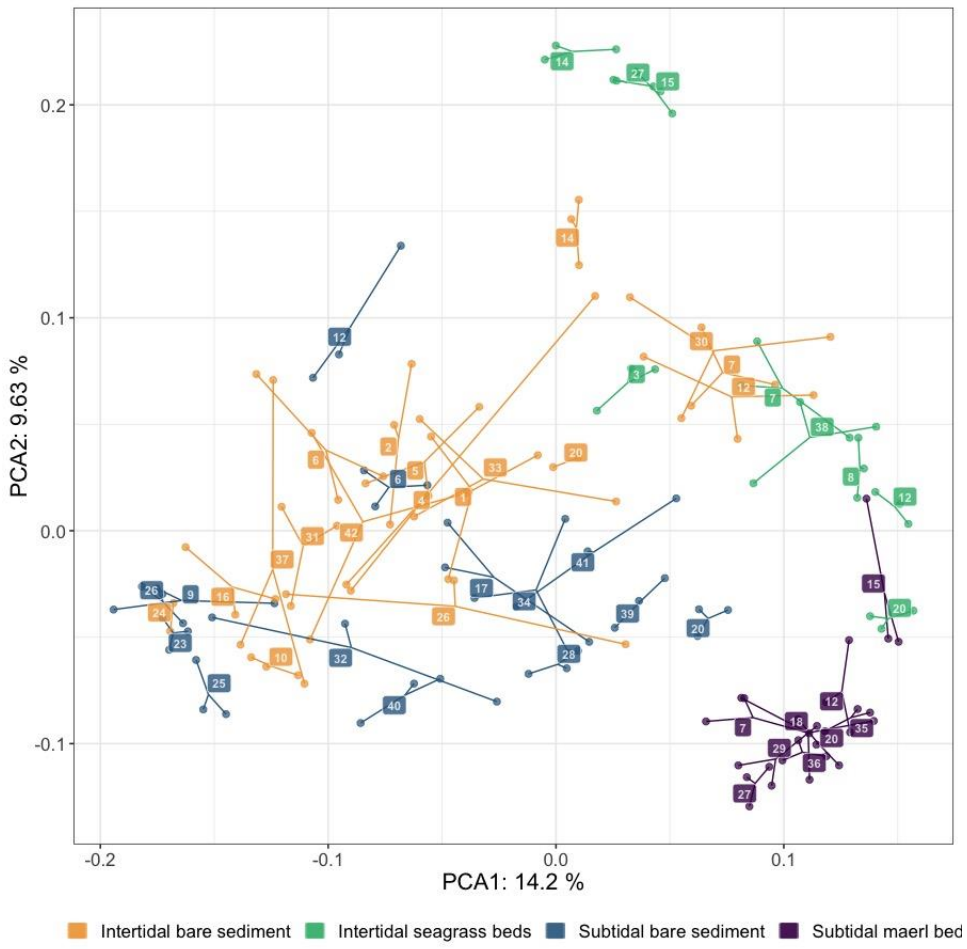

Figure S3 Alternative representation of the principal component analysis of Hellinger-transformed polychaete abundances represented in Figure 2 in the main text. Samples are displayed in scaling 1 and species are omitted. A point represents the position of a community of a given site for a given year. The lines link the position of the communities of a site at each year to the centroid position of the same community across years. This illustrates within-site dispersion and represents the community's temporal variability. Colours correspond to the habitats. Sites are labelled as in Figure S1 to identify the centroid position of each site for the different habitats. A given site may harbour different habitats (e.g. site 7, 12 and 14)

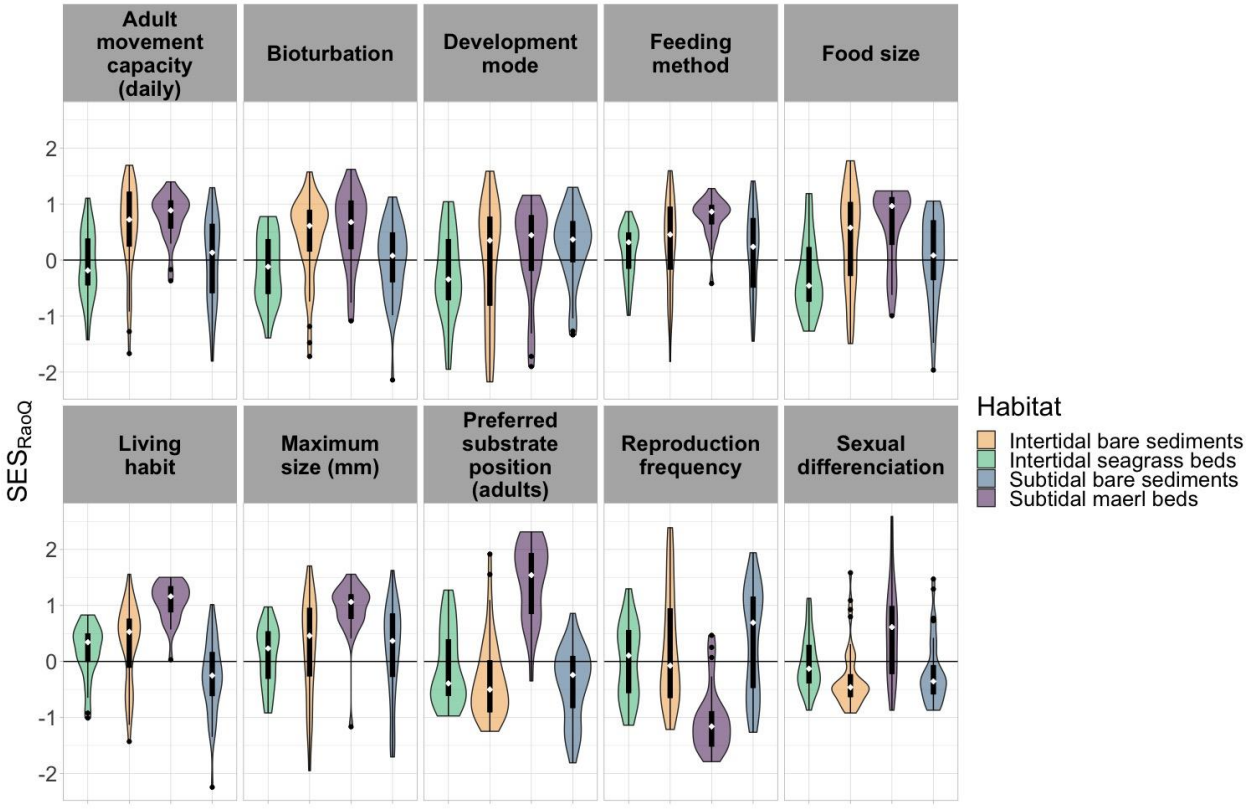

Figure S4 Distribution of the SES values for each trait individually. Positive SES values indicate trait divergence, while negative values suggest trait convergence. Near zero values indicate random distribution. Values of Rao's quadratic entropy were calculated for each trait separetely and compared to null expectations using randomisation of the communities. For further details please refer to the Material and Methods section of the article

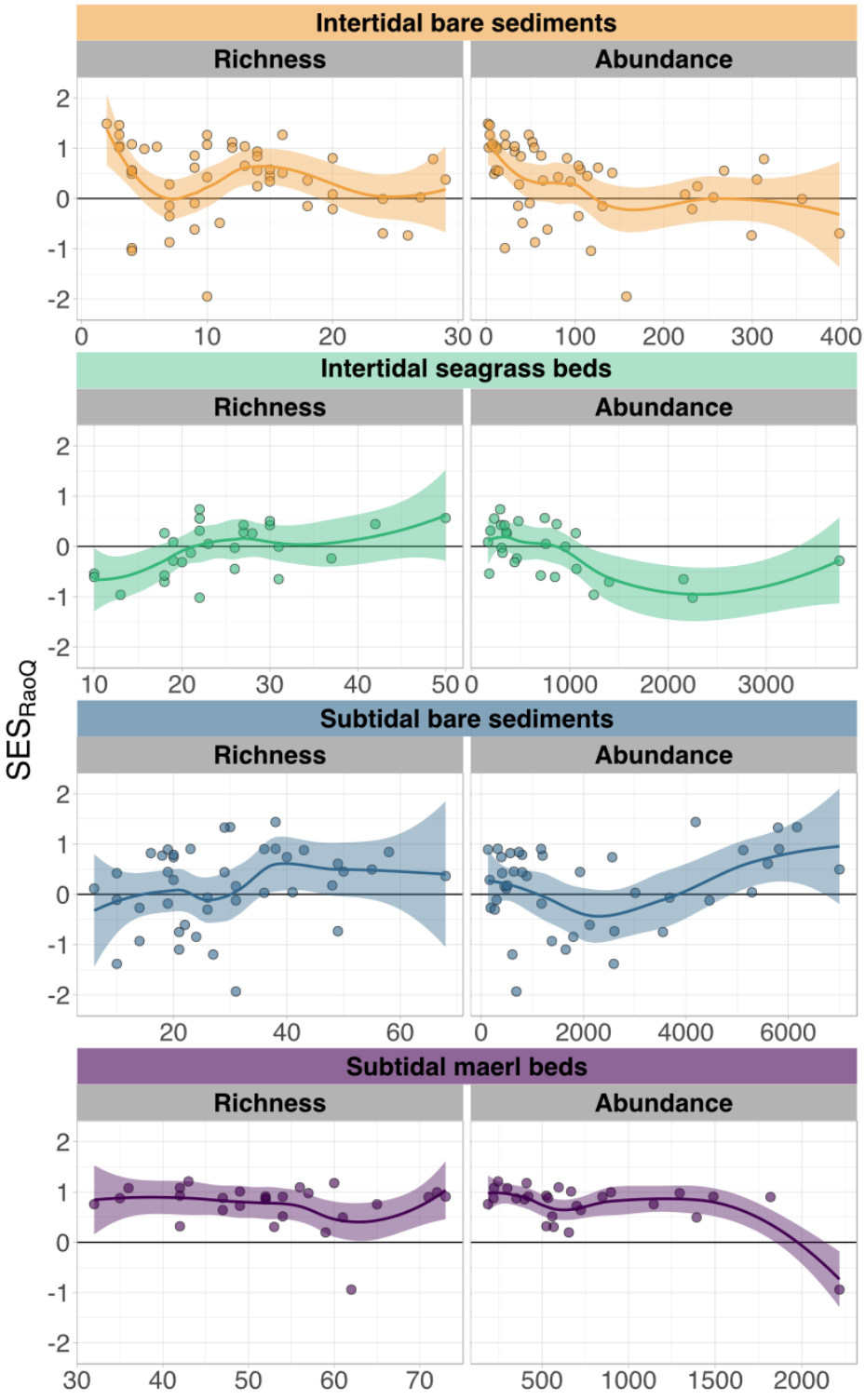

Figure S5 Relationships between the SES_{RaoQ} and the richness or total abundance of the assemblages for the four habitats

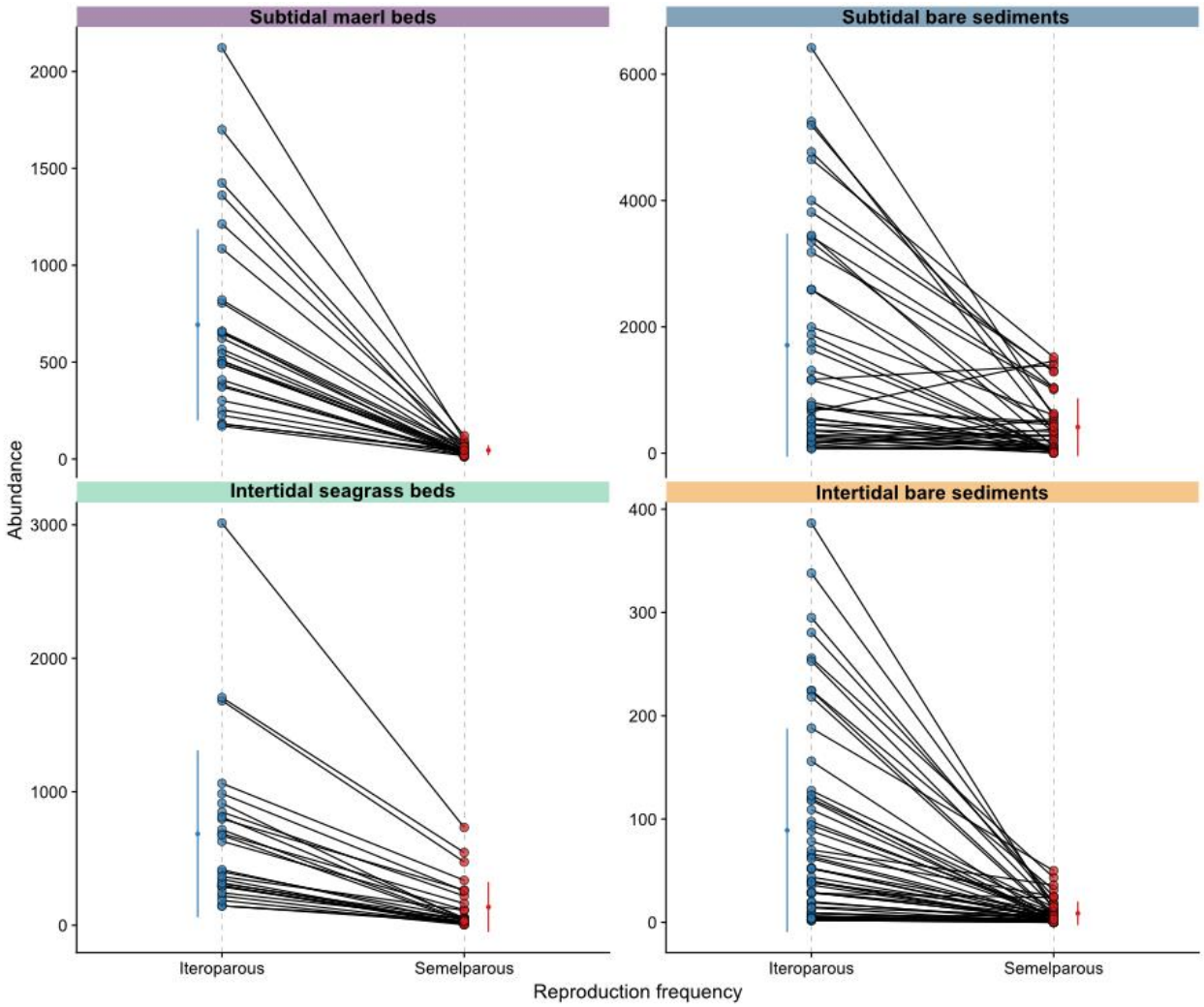

Figure S6 Abundances of the two modalities of reproduction frequency for the different assemblages of each habitat. The lines link the abundance of one modality to the abundance of the other for each assemblage. The mean and standard deviation of each modality for each habitat are plotted next to the points. For subtidal maerl assemblages, reproduction frequency consistently converge towards iteroparous species while the distribution of abundances among the two modalities is more variable and in general follow a random pattern in the other habitats (see Figure S3)

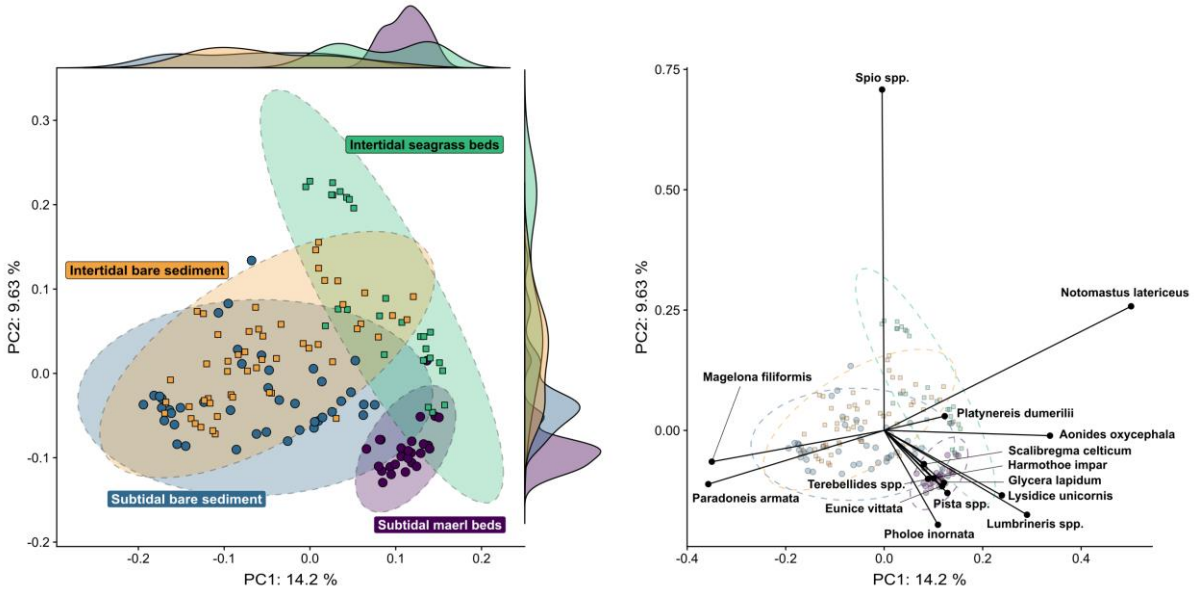

Figure S7 Principal component analysis of Hellinger-transformed polychaete abundances. Left panel: Samples are displayed on the central panel in scaling 1 (this panel is the same figure shown in Figure 2 in the main text). The shapes of the points reflect differences in the tidal levels and sampling methods: squares represent intertidal habitats sampled using sediment cores and circles represent subtidal habitats sampled using grabs. The density of points for each habitat along the first and second axis are displayed in the outer panels. Within-habitat variability comprises of both spatial and temporal variations (see Figure S1). The first two axes represented account for 23.83% of the total variance of polychaete composition. Right panel: only the species whose variance in these two axes represents more than 30% of their total variance are represented (assessed with the function goodness; vegan)

7. References

Blonder, B. (2017). Hypervolume concepts in niche- and trait-based ecology. *Ecography*, *40*, 001–013. https://doi.org/10.1111/ecog.03187

Bouma, T. J., Olenin, S., Reise, K., & Ysebaert, T. (2009). Ecosystem engineering and biodiversity in coastal sediments: Posing hypotheses. *Helgoland Marine Research*, *63*(1), 95–106. http://doi.org/10.1007/s10152-009-0146-y

Boyé, A., Legendre, P., Grall, J., & Gauthier, O. (2017). Constancy despite variability: Local and regional macrofaunal diversity in intertidal seagrass beds. *Journal of Sea Research*, *130*, 107–122. https://doi.org/https://doi.org/10.1016/j.seares.2017.06.004

Cornwell, W. K., Schwilk, D. W., & Ackerly, D. D. (2006). A trait-based test for habitat filtering: Convex hull volume. *Ecology*, *87*(6), 1465–1471. https://doi.org/10.1890/0012-9658(2006)87[1465:attfhf]2.0.co;2

Degen, R., Aune, M., Bluhm, B. A., Cassidy, C., Kędra, M., Kraan, C., Vandepitte, L., Włodarska-Kowalczuk, M., Zhulay, I., Albano, P. G. , Bremner, J., Grebmeier, J. M., Link, H., Morata, N., Nordström, M. C., Shojaei, M. G., Sutton, L., & Zuschin, M. (2018). Trait-based approaches in rapidly changing ecosystems: A roadmap to the future polar oceans. *Ecological Indicators*, *91*, 722–736. http://doi.org/10.1016/j.ecolind.2018.04.050

Kowarik, A., & Templ, M. (2016). Imputation with the R package VIM. *Journal of Statistical Software*, *74*(7), 1–16. https://doi.org/10.18637/jss.v074.i07

Laliberté, E., & Legendre, P. (2010). A distance-based framework for measuring functional diversity from multiple traits. *Ecology*, *91*(1), 299–305. https://doi.org/10.1890/08-2244.1

Legendre, P., & Legendre, L. (2012). *Numerical ecology, 3rd english edition*. Elsevier.

Mouchet, M. A., Villéger, S., Mason, N. W. H., & Mouillot, D. (2010). Functional diversity measures: An overview of their redundancy and their ability to discriminate community assembly rules. *Functional Ecology*, *24*(4), 867–876. https://doi.org/10.1111/j.1365-2435.2010.01695.x

Norling, K., Rosenberg, R., Hulth, S., Grémare, A., & Bonsdorff, E. (2007). Importance of functional biodiversity and species-specific traits of benthic fauna for ecosystem functions in marine sediment. *Marine Ecology Progress Series*, *332*(2004), 11–23. http://doi.org/10.3354/meps332011

Queirós, A. M., Birchenough, S. N. R., Bremner, J., Godbold, J. A., Parker, R. E., Romero-Ramirez, A., Reiss, H., Solan, M., Somerfield, P. J., Van Colen, C., Van Hoey, G., & Widdicombe, S. (2013). A bioturbation classification of European marine infaunal invertebrates. *Ecology and Evolution*, *3*(11), 3958–3985. http://doi.org/10.1002/ece3.769

Schleuter, D., Daufresne, M., Massol, F., & Argillier, C. (2010). A user's guide to functional diversity indices. *Ecological Monographs*, *80*(3), 469–484. https://doi.org/10.1890/08-2225.1

Törnroos, A., & Bonsdorff, E. (2012). Developing the multitrait concept for functional diversity: Lessons from a system rich in functions but poor in species. *Ecological Applications*, *22*(8), 2221–2236. http://doi.org/10.1890/11-2042.1

Villéger, S., Mason, N. W., & Mouillot, D. (2008). New multidimensional functional diversity indices for a multifaceted framework in functional ecology. *Ecology*, *89*(8), 2290–2301. https://doi.org/https://doi.org/10.1890/07-1206.1

Wohlgemuth, D., Solan, M., & Godbold, J. A. (2017). Species contributions to ecosystem process and function can be population dependent and modified by biotic and abiotic setting. *Proceedings of the Royal Society B: Biological Sciences*, *284*(1855), 20162805. https://doi.org/10.1098/rspb.2016.2805